Available online at www.sciencedirect.com
SCIENCE DIRECT®

Chemical Physics 296 (2004) 273–279

Chemical Physics

www.elsevier.com/locate/chemphys

Optimizing terahertz emission from double quantum wells ☆

Ke Dong [a], Nancy Makri [a,b,*]

[a] Department of Physics, University of Illinois, 1110 West Green Street, Urbana, IL 61801, USA
[b] Department of Chemistry, University of Illinois, 601 South Goodwin Avenue, Urbana, IL 61801, USA

Received 4 July 2003; accepted 17 September 2003

Abstract

The terahertz (THz) radiation emitted from a double quantum well is investigated and optimized. Exploiting the phenomenon of quantum stochastic resonance (whereby the oscillation amplitude of a dissipative two-level system exhibits at low temperatures a non-monotonic response with respect to the parameters of a monochromatic external field or the strength of dissipation) to drive a series of identical double quantum wells, it is shown that the coherence properties of the emitted THz radiation can be boosted significantly.

1. Introduction

Electromagnetic radiation in the terahertz frequency range has been observed experimentally in both single [1] and double [2,3] GaAs/AlGaAs quantum well structures. In the case of a dc-biased asymmetric double quantum well (DQW) of the type shown in Fig. 1, a short laser pulse can pump electrons coherently into the two conduction subbands. The electrons tunnel back and forth between the wide well (WW) and the narrow well (NW) with a frequency corresponding to the tunneling splitting between the two conduction subbands, generating a time-varying polarization. The electromagnetic radiation generated from this polarization is usually in the THz range. Dephasing effects arising mainly from intercarrier Coulomb interactions lead to damping usually within several picoseconds [1–3].

In recent years there has been great interest in the quantum control of THz emission. For example, using pairs of phase-locked femtosecond laser pulses Planken et al. have theoretically [4] and experimentally [5] demonstrated that THz radiation signals generated from dc-biased asymmetric DQWs can be enhanced, weakened, or phase-shifted by adjusting the relative phase and time delay between the optical pulses.

The present work aims at optimizing the THz radiation emitted from DQW structures by utilizing novel features of the quantum stochastic resonance (QSR) phenomenon [6–13]. QSR in a dissipative two-level system (TLS) was originally studied in the regime of small dissipation and weak external fields [7]. At resonant driving, QSR manifests itself as a non-monotonic response of the long-time TLS oscillation amplitude to the strength of dissipation or the amplitude of the driving field, and optimal response is achieved at a field amplitude proportional to the TLS relaxation rate. This earlier work in the weak field regime predicted a single maximum of the TLS steady-state oscillation amplitude, which is a function of temperature only and independent of bath properties. In this regime increase of the external field strength above the optimal value leads to a monotonic decrease of the TLS oscillation amplitude.

We recently extended the early work to strong external fields [14]. Our calculations revealed the existence of interesting patterns in the long-time oscillation amplitude of the system that vary with the external field parameters. These effects lead to a more complex dependence of the steady-state TLS oscillation amplitude on field strength and driving frequency, suggesting a multitude of “optimal driving” conditions.

☆ Dedicated to the 60th birthday of Ulrich Weiss.

* Corresponding author. Tel.: +1-217-333-6589; fax: +1-217-244-0789.
E-mail address: nancy@scs.uiuc.edu (N. Makri).

0301-0104/$ - see front matter © 2003 Elsevier B.V. All rights reserved.
doi:10.1016/j.chemphys.2003.09.016

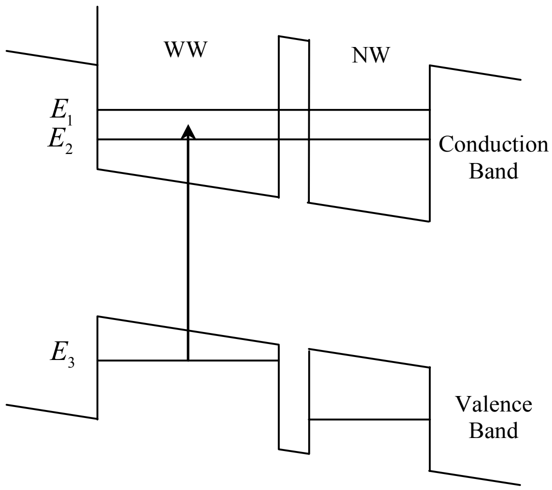

Fig. 1. Schematic band diagram of the biased asymmetric double quantum well. A coherent excitation of electrons into the E_1 and E_2 levels of the conduction band results in a time-varying polarization as the charges tunnel back and forth between WW and NW.

Borrowing the concept of "friction" to simulate dephasing effects in dc-biased asymmetric DQWs maps the dynamics within the conduction subbands to that of a dissipative TLS. We use the short-lived THz radiation emitted from a DQW to drive a second DQW. At favorable values of the parameters, the phenomenon of QSR leads to enhancement of the emitted THz signal from the second DQW. Repeating the procedure can lead to further boosting of the THz signal in each successive step of the cycle. It can be shown that long-lived and robust THz signals can be generated this way.

Our simulations are based on the path integral formulation of time-dependent quantum mechanics. Observables relevant to the TLS dynamics are obtained from the TLS reduced density matrix. Employing a harmonic bath model to mimic the effects of dissipation and influence functional obtained by Feynman and Vernon [15] leads to path integral expressions for the TLS reduced density matrix that involve non-local two-time correlations which resemble memory effects in the classical generalized Langevin description of a system interacting with a dissipative environment. Evaluation of the path integral is possible using methodology developed earlier in our group. This exploits the finite length of non-local in time correlations in the influence functional of a dissipative environment to propagate time-dependent quantities through an iterative procedure.

Section 2 describes the theoretical models and various numerical procedures that we use. The same section reviews the phenomenon of QSR. Section 3 presents the numerical results, and Section 4 summarizes the findings of this work.

2. Background

While the application of a dc-biased field can cause the electron levels in the conduction subbands to move into tunneling resonance, the heavy-hole levels in the valence band diverge in energy as the dc field increases and are therefore mostly localized for a large range of field strengths. As a result, if the spectral bandwidth of the pumping laser field applied to the DQW system is larger than the energy splitting between the lowest two coupled conduction subbands of the WW and NW but small compared to the energy difference between the top two heavy-hole energy levels in the valence band, one can reasonably assume that there is no contribution from all the valence subbands except the top heavy-hole level in the WW. As a consequence, one can use a single-particle, effective-mass picture to describe the dynamics of the biased DQW system, which involves only one heavy-hole level in the valence band and two electron levels in the conduction band. The corresponding time-dependent Hamiltonian can be written as [16]

$$\hat{H}_0(t) = \hat{H}_{\mathrm{TLS}} + E_0|0\rangle\langle 0| - \varepsilon(t)(\mu_{01}|0\rangle\langle 1| + \mu_{10}|1\rangle\langle 0| + \mu_{02}|0\rangle\langle 2| + \mu_{20}|2\rangle\langle 0|), \tag{1}$$

where

$$\hat{H}_{\mathrm{TLS}} = E_1|1\rangle\langle 1| + E_2|2\rangle\langle 2|. \tag{2}$$

Here $\hat{H}_{\mathrm{TLS}}$ is the Hamiltonian for the electron states, μ_{01} and μ_{02} are the transition dipole moments between the heavy-hole state and the electron states, and $\varepsilon(t)$ is the external laser field. When a short laser pulse pumps electrons coherently into the conduction subbands, the charges tunneling back and forth between the two wells with a frequency corresponding to the energy splitting between the two bands generate a time-varying polarization, which (ignoring the high-frequency components) can be expressed using a density matrix formulation as

$$P(t) \propto [(\mu_{11} - \mu_{00})\rho_{11}(t) + (\mu_{22} - \mu_{00})\rho_{22}(t) + \mathrm{Re}(\mu_{21}\rho_{12}(t) + \mu_{12}\rho_{21}(t))], \tag{3}$$

where μ_{ii} are the self-dipole moments, and μ_{12} and μ_{21} are the transition dipole moments between the electron states. In the last equation ρ_{11} and ρ_{22} are the generated electron densities in the two conduction subbands, while the off-diagonal terms ρ_{12} and ρ_{21} describe the coherence between them. In turn, the time-dependent polarization $P(t)$ leads to dipole radiation with an electromagnetic field

$$\varepsilon_{\mathrm{THz}}(t) \sim \frac{\partial^2 P(t)}{\partial t^2}. \tag{4}$$

In the absence of additional external driving, the emission frequency is determined by the tunneling splitting between the two electron levels and therefore can be tuned by adjusting the magnitude of the dc field or by changing the dimension of the asymmetric DQW.

A coherent superposition of the two electron states in the conduction band is created by using a two-frequency field to excite the $|0\rangle \to |1\rangle$ and $|0\rangle \to |2\rangle$ transitions or, equivalently, by applying a Gaussian laser field centered about the frequency $\hbar\omega_{\rm exc} = (E_1 + E_2)/2 - E_0$ with a bandwidth that equals or exceeds the tunneling splitting. This superposition corresponds to a localized charge state whose tunneling oscillations lead to THz radiation. Once the pumping excitation field is turned off, only the tunneling process between the two electron states $|1\rangle$ and $|2\rangle$ is operative. Decoherence due to inter-carrier Coulomb interactions causes the decay of the emitted radiation, typically within a few oscillation periods [1–3].

Pötz [17] has given a non-phenomenological microscopic analysis of THz emission by laser-induced charge oscillations in asymmetric GaAs/AlGaAs double well systems. That study considered the destruction of phase coherence due to the inter-carrier Coulomb interaction and concluded that the generated electric field could be fitted by an exponentially damped trigonometric function. It is well-known that the tunneling process in a two-level system coupled to a harmonic dissipative bath with Ohmic dissipation is also characterized by an exponentially damped trigonometric function in the low temperature and weak friction regime [18]. Hence one may use the concept of "friction" to simulate the decoherence process due to the charge carrier dynamics in the two electron levels. As a consequence, the tunneling process along with the coherence decay can be sufficiently modeled by the so-called "spin-boson" Hamiltonian, which consists of a TLS coupled bilinearly to a dissipative bath of harmonic oscillators

$$\hat{H}_{\rm SB} = -\frac{1}{2}\hbar\Omega\hat{\sigma}_x + \sum_j \left(\frac{p_j^2}{2m_j} + \frac{1}{2} m_j \omega_j^2 x_j^2 \right) + q_0 \sum_j c_j x_j \hat{\sigma}_z. \tag{5}$$

Here $\hat{\sigma}_x = |L\rangle\langle R| + |R\rangle\langle L|$ and $\hat{\sigma}_z = |R\rangle\langle R| - |L\rangle\langle L|$ are operators corresponding to the Pauli spin-1/2 matrices in the basis of the TLS "left" and "right"-localized states

$$|L\rangle = \frac{1}{\sqrt{2}}(|1\rangle + |2\rangle), \quad |R\rangle = \frac{1}{\sqrt{2}}(|1\rangle - |2\rangle), \tag{6}$$

$\hbar\Omega = E_2 - E_1$ is the TLS tunneling splitting, and $2q_0$ is the distance between the two wells.

The characteristics of the bath affecting the system dynamics are described by the spectral density function

$$J(\omega) = \frac{\pi}{2} \sum_j \frac{c_j^2}{m_j \omega_j} \delta(\omega - \omega_j). \tag{7}$$

Condensed phase environments give rise to continuous spectral densities and lead to dissipative dynamics characterized by the destruction of the TLS coherence. In the present study we employ the model of an Ohmic bath, with a spectral density given by the expression

$$J(\omega) = \eta\omega e^{-\omega/\omega_c}, \tag{8}$$

where η is the friction coefficient and ω_c is the bath cutoff frequency [18]. The strength of friction is quantified by the dimensionless Kondo parameter $\alpha = 2\eta q_0^2/\pi\hbar$. External driving of the electronically excited doublet is described by including a time-dependent term in Eq. (5) of the type

$$\hat{H}_{\rm ext}(t) = \sigma_z V(t). \tag{9}$$

Time-dependent observables can be obtained from the TLS reduced density operator,

$$\hat{\rho}_{\rm red}(t) = {\rm Tr}_{\rm bath}(\hat{U}(t)\hat{\rho}(0)\hat{U}(t)^{-1}), \tag{10}$$

where $\hat{U}(t)$ is the time evolution operator for the composite time-dependent Hamiltonian

$$\hat{H}(t) = \hat{H}_{\rm SB} + \hat{H}_{\rm ext}(t). \tag{11}$$

For simplicity we use a "factorized initial condition",

$$\hat{\rho}(0) = |R\rangle\langle R| e^{-\beta\hat{H}_{\rm bath}} / {\rm Tr}\, e^{-\beta H_{\rm bath}}, \tag{12}$$

where $H_{\rm bath}$ is the TLS-independent part of Eq. (5), i.e., assume that the TLS is initially uncorrelated from the bath, which is at thermal equilibrium at the temperature $T = 1/k_{\rm B}\beta$, where is the Boltzmann constant. The complex behaviors that characterize the long-time oscillation amplitude in dissipative TLSs driven by monochromatic fields have been the subject of numerous experimental and theoretical investigations [6,8–13].

Feynman and Vernon [15] have shown that the reduced density matrix for Eq. (10) can be expressed in terms of a path integral for the system of interest augmented with an influence functional. In the case of a harmonic bath, the latter is a Gaussian functional of TLS paths with non-local two-time coefficients given by the bath correlation function, which are known to eventually decay to zero when the environment is characterized by a continuous spectral density arising from an infinite number of degrees of freedom. These two-time correlations are analogous to memory effects in the classical generalized Langevin equation [19] for a system interacting with a dissipative environment [20]. Earlier work in our group exploited this structure to devise an iterative procedure for the evaluation of the reduced density matrix. Specifically, discretization of the path integral through the use of a finite time step and truncation of the non-local interactions allows evaluation of the path integral for the reduced density matrix by a matrix multiplication procedure with an effective propagator which connects path segments that span the memory length [7,21–25]. The method converges easily, provided that the memory time of the bath is not very long compared to the shortest time scale in the Hamiltonian that dictates the maximum allowed time step. Similar iterative procedures have been developed for equilibrium two- or multi-time correlation functions corresponding to non-factorized initial conditions [26,27]. It has also been shown [28] that an iterative formulation is possible in the case of a general anharmonic environment using numerical procedures to evaluate the influence functional.

Consider driving the TLS by a monochromatic field given by the function

$$V(t) = V_0 \cos \omega t. \tag{13}$$

Using the quantized representation of this radiation field the total Hamiltonian $\hat{H}(t)$ for the driven dissipative TLS can be written in the following time-independent form

$$\hat{H}_{\mathrm{SFB}} = -\frac{1}{2}\hbar\Omega\hat{\sigma}_x + g\hat{\sigma}_z(\hat{a}^+ + \hat{a}) + \hbar\omega\hat{a}^+\hat{a} + \frac{g^2}{\hbar\omega} + \sum_j \left[\frac{p_j^2}{2m_j} + \frac{1}{2}m_j\omega_j^2x_j^2 + c_jx_jq_0\hat{\sigma}_z\right], \tag{14}$$

where $\hat{a}^+$ and $\hat{a}$ are photon creation and annihilation operators. For the time-dependent and quantized field representations to describe the same physical situation the coupling energy between TLS and field must satisfy the relation $g = V_0/\sqrt{2(2n+1)}$, where n is the quantum number specifying the photon state [29]. Eq. (14) describes a curve crossing system of two harmonic oscillators interacting with a harmonic bath and thus can be rewritten in the following equivalent form [30],

$$\hat{H}_{\mathrm{SFB}} = \sum_{m=0}^{\infty} \hat{H}^{(m)} + \hat{H}_{\mathrm{cross}}, \tag{15}$$

where

$$\hat{H}^{(m)} = \left[m\hbar\omega + \sum_j \left(\frac{p_j^2}{2m_j} + \frac{1}{2}m_j\omega_j^2x_j^2\right)\right]\hat{I}^{(m)} - \frac{1}{2}\hbar\Omega_m\hat{\sigma}_x^{(m)} + \sum_j c_jx_jq_0\hat{\sigma}_z^{(m)}, \tag{16}$$

$$\begin{aligned}
\hat{I}^{(m)} &= |\tilde{L}_m\rangle\langle\tilde{L}_m| + |\tilde{R}_m\rangle\langle\tilde{R}_m|,\\
\hat{\sigma}_x^{(m)} &= |\tilde{L}_m\rangle\langle\tilde{R}_m| + |\tilde{R}_m\rangle\langle\tilde{L}_m|,\\
\hat{\sigma}_z^{(m)} &= |\tilde{L}_m\rangle\langle\tilde{L}_m| - |\tilde{R}_m\rangle\langle\tilde{R}_m|,\\
|\tilde{L}_n\rangle &= \mathrm{e}^{-\xi(\hat{a}^+ - \hat{a})}|n\rangle \otimes |L\rangle,\\
|\tilde{R}_n\rangle &= \mathrm{e}^{\xi(\hat{a}^+ - \hat{a})}|n\rangle \otimes |R\rangle, \quad \xi = g/\hbar\omega,\\
\Omega_m &= \Omega\langle m|\exp(\xi(\hat{a}^+ - \hat{a}))|m\rangle, \quad \hat{\sigma}_z = \sum_{m=0}^{\infty}\hat{\sigma}_z^{(m)}.
\end{aligned} \tag{17}$$

The first part of Eq. (15) describes an infinite series of independent tunneling doublets with intradoublet splitting $\hbar\Omega_m$ and interdoublet spacing $\hbar\omega$, with each doublet coupled to a replica of the same harmonic bath; interdoublet coupling terms are collected in $\hat{H}_{\mathrm{cross}}$, which can be considered a perturbation in the case of high-frequency driving, $\omega \gg \Omega$. Typical (strong) radiation fields correspond to $n \gg 1$ and $\sqrt{n}g \gg \hbar\Omega$ [30]. Ignoring the interdoublet coupling terms it follows that the driven TLS is equivalent to a new TLS with a renormalized tunneling splitting $\Omega_{\mathrm{eff}} = \Omega|J_0(2V_0/\hbar\omega)|$, where J_0 is the zeroth order Bessel function [10,31,32]. In the present paper we are interested in the behavior of Eq. (15) in the damped oscillation regime corresponding to $0 < \alpha < 1/2$ and $\alpha T < \Omega(\Omega/\omega_c)^{\alpha/(1-\alpha)}$. In this regime the driven system can cross over from underdamped to exponential decay dynamics depending on the relation between αT and $\Omega_{\mathrm{eff}}(\Omega_{\mathrm{eff}}/\omega_c)^{\alpha/(1-\alpha)}$ [18].

Dissipation is generally associated with the destruction of coherence. As an exception to that conventional wisdom, stochastic resonance in bistable systems is an intriguing phenomenon where the response of driven systems with persistent coherences is enhanced due to the collective cooperation between random noise, bistability, and periodic forcing [6–13,33,34]. At zero temperature only quantum stochastic resonance survives, and the non-linear response of a driven quantum mechanical system originates in quantum noise [6–13]. QSR in TLSs has been studied in the limit of small dissipation and weak fields [7]. In that regime the average position of the driven TLS exhibits undamped oscillatory motion at long times whose amplitude is enhanced by friction. Fig. 2 shows the results of accurate path integral calculations that illustrate this behavior for the case of resonant driving ($\omega = \Omega$). These calculations were performed at two values of friction with the field amplitude $V_0 = 0.1\Omega$, the cutoff frequency of the bath $\omega_c = 8.256\Omega$, and the system inverse temperature $\beta = 5.813\,\hbar\Omega$. Converged results were obtained by choosing the path integral time step $\Delta t = 0.08(2\pi\Omega)$ and

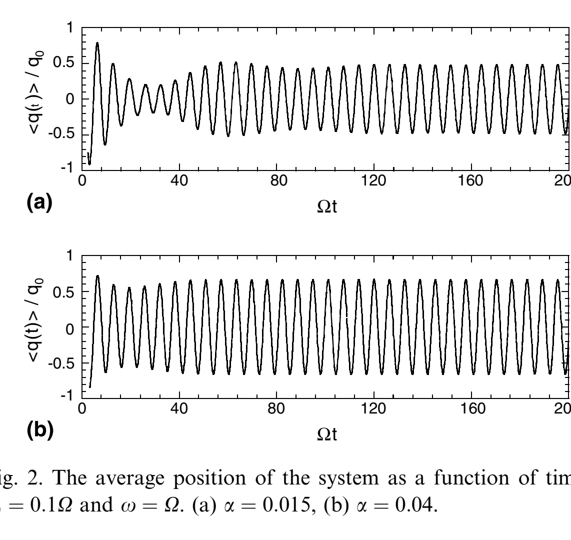

Fig. 2. The average position of the system as a function of time for $V_0 = 0.1\Omega$ and $\omega = \Omega$. (a) $\alpha = 0.015$, (b) $\alpha = 0.04$.

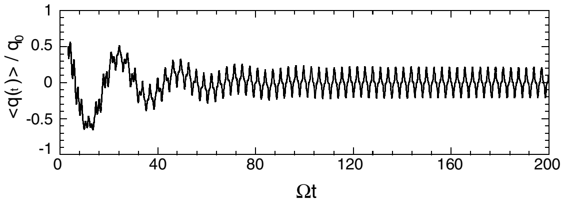

Fig. 3. The average position of the system as a function of time for $V_0 = 3\Omega, \omega = 2\Omega$ and $\alpha = 0.04$.

including non-local influence functional interactions over a range equal to $6\Delta t$.

In a recent paper [14] we investigated the QSR phenomenon over a larger range of driving field strengths and frequencies, and found a much richer structure compared to that reported in the weak field limit [7]. Fig. 3 shows the TLS average position for $\omega = 2\Omega$, $V_0 = 3\Omega$ and $\alpha = 0.04$. One observes high-frequency components in the TLS oscillation at long times, which can be attributed to a concerted effort by the bistable system, the driving field and the harmonic bath. In order to demonstrate the relationship between the QSR in the weak and strong field limits we plot in Fig. 4 the long time oscillation amplitude $q_{\max}$ at resonant driving ($\omega = \Omega$) as a function of the Kondo parameter α over a range of field strengths that span both regimes. One observes that the QSR peak shifts to the right with increasing field amplitude. It is seen that the QSR previously characterized for weak fields persists in the strong field regime, where the TLS dynamics displays more complex behaviors.

The steady-state TLS oscillation amplitude exhibits an interesting non-monotonic dependence on field strength displayed in Fig. 5. In addition to the maximum

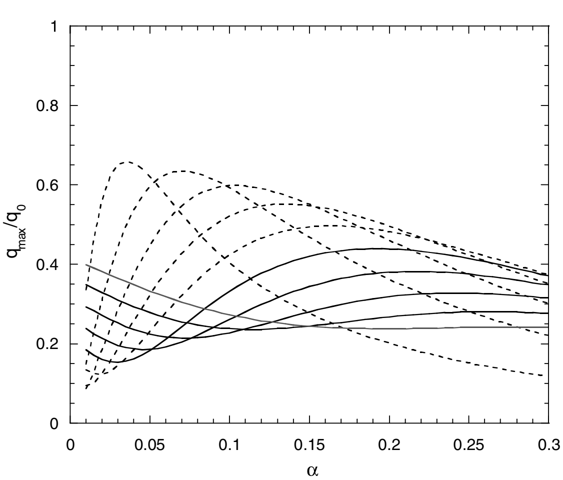

Fig. 4. Dependence of the long-time oscillation amplitude on the Kondo parameter at resonant driving ($\omega = \Omega$). Curves with peaks from left to right correspond to $2V_0/\hbar\Omega$ values between 0.2 and 2.0, in increments of 0.2. The transition from the weak (dashed lines) to the strong (solid lines) regime is clearly seen.

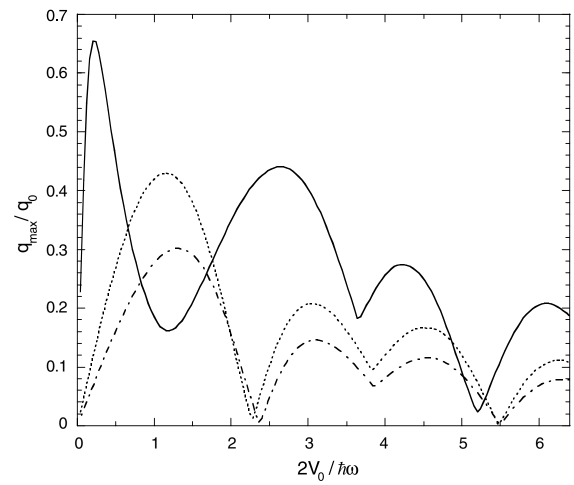

Fig. 5. The amplitude of coherent oscillation as a function of $2V_0/\hbar\omega$ when $\alpha = 0.04$. The oscillation amplitude is recorded from the peak nearest to $t = 80 \times 2\pi/\Omega$, for three different driving frequencies. The oscillation amplitudes show similar “interference patterns”. Solid line: $\omega = \Omega$. Dotted line: $\omega = 2\Omega$. Chain-dotted line: $\omega = 3\Omega$.

at resonant driving displayed in the weak field region, the steady-state oscillation amplitude displays numerous secondary peaks, local minima, and zeros. Notably, the system’s behavior at $\omega = \Omega$ is markedly different from all the others, a clear manifestation of the breakdown of the perturbation theory, and its first peak corresponds to the QSR at the weak field and small dissipation limit identified in [7].

3. Amplification of THz emission

The double quantum well system we will consider below consists of a wide well of 145 Å and a narrow well of 100 Å, separated by a 25-Å thick $Al_xGa_{1-x}As$ barrier [3]. In the following, the calculations are performed using the 57:43 conduction [35], the effective masses are assumed to be $0.330m_e$ and $0.0665m_e$ for the heavy holes and electrons, respectively, and the confining potentials are 228 and 172 meV for the conduction and valence bands, respectively. The energy gap between the top of the valence band and the bottom of the Γ-valley of the conduction band is taken to be 1.519 eV. For this configuration the splitting between the two conduction subbands shows a nearly parabolic dependence on the dc field strength, centered around 10 kV/cm with the corresponding minimum at about 5 meV or 1.2 THz. Without losing generality, we will use a dc field of 11 kV/cm throughout this paper, which corresponds to the tunneling splitting $\Omega = 1.211$ THz. The long-time dynamics of the driven dissipative TLS was calculated in all cases using the iterative path integral methodology discussed in the previous section. The calculations were performed at the temperature $T = 10$ K ($\hbar\Omega\beta = 5.813$).

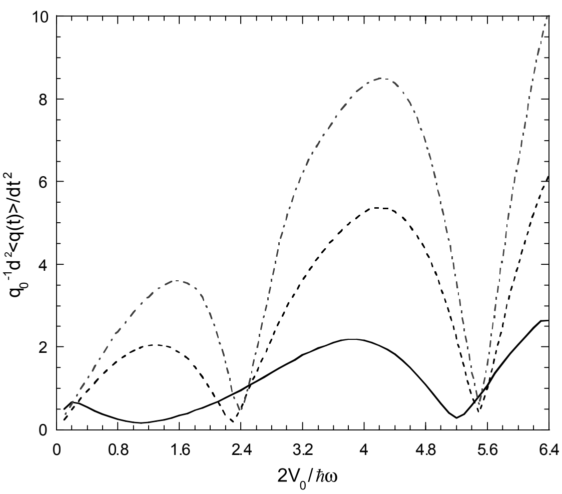

Fig. 6. The amplitude of THz signals as a function of $2V_0/\hbar\omega$ when $\alpha = 0.04$. The oscillation amplitude is recorded from the peak nearest to $t = 80 \times 2\pi/\Omega$, for three different driving frequencies, $\omega = \Omega$ (solid line), 2Ω (dashed line) and 3Ω (chain-dotted line).

As explained in the introduction section, the bath parameters are obtained by fitting the simulation results of Pötz [17] to available expressions for dissipative two-level system dynamics. Using a damping time of 2.02 ps and an oscillation frequency of 0.89 THz [17], the Kondo parameter and the cutoff frequency are estimated to be about $\alpha = 0.05$ and $\omega_c = 8.256\Omega = 10$ THz, respectively. Furthermore, it was found [36] in a similar double quantum well system that the dephasing time is almost the same for excitation densities below 10^{10} cm^{-2}. As a result, when we change the strength of the input laser field we assume that the Kondo parameter α and cutoff frequency ω_c remain unchanged as long as the resulting excitation density is small.

Fig. 6 displays the maximum steady-state amplitude of the emitted radiation as a function of the driving field parameters. These results were obtained using numerical derivative procedures to calculate the second derivative of the numerical path integral results for the TLS average position. One observes large secondary and tertiary peaks of growing magnitude. In particular, the emitted signal exhibits a very large amplification at driving frequencies higher than the TLS splitting. This effect arises from the high frequency components of the TLS dynamics in the strong field regime, which are magnified by a factor of ω^2 through the second derivative operation.

The non-linear dependence of the long-time oscillation amplitude on driving field strength can be exploited to further boost the THz signal. This is demonstrated with the following idealized experiment: Consider a series of identically prepared asymmetric DQWs (see Fig. 7(a)) labeled $i = 1, 2, \ldots$ We assume that when the front of the THz signal originating from DQW i arrives at DQW $i+1$ at time t_{i+1}, the asymmetric DQW at site i

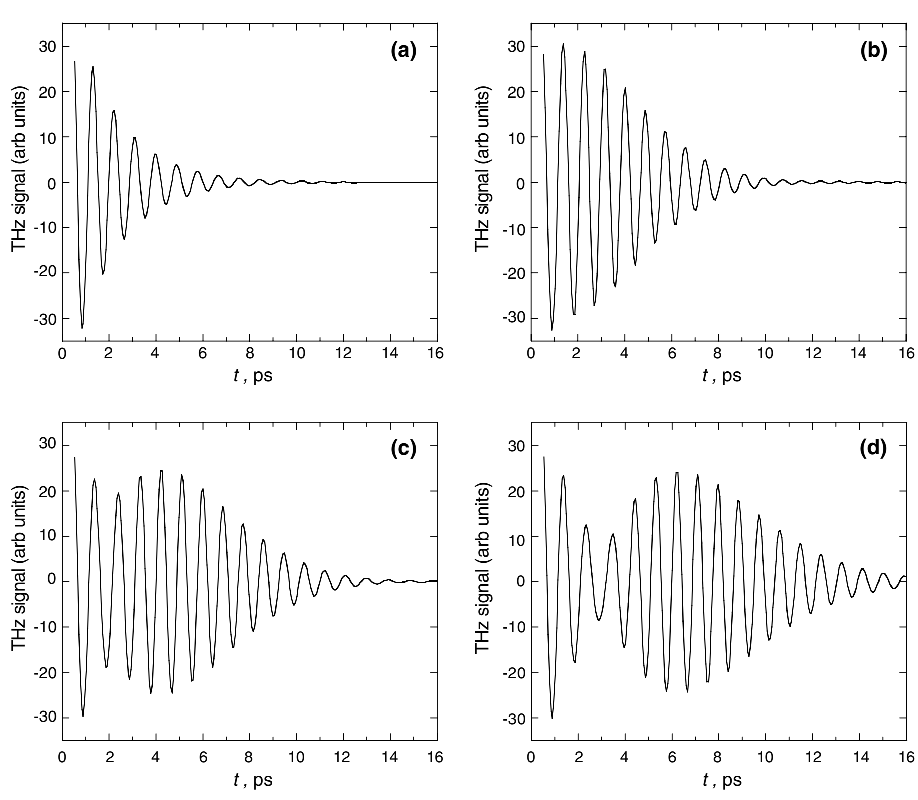

Fig. 7. The THz signal at sight i. The asymmetric DQWs are so prepared that when the resonant driving field from site $i-1$ arrives at site i at time t_i, $\langle q_i(t_i)\rangle = q_0$.

is prepared in the right-localized state, i.e., $\langle q^{(i+1)}(t_{i+1})\rangle = q_0$. In addition, we assume that radiation generated from DQW I induces on the tunneling charges of DQW i+1 an electric field with an amplitude $0.115\hbar\Omega/\mu_{12}$ (where μ_{12} is the dipole moment associated with the tunneling doublet). This field amplitude corresponds to maximum TLS oscillation at the assumed friction value described earlier in this section. No external control field is applied to the first of these DQWs, for which the computed emitted THz radiation is shown in Fig. 7(a).

As discussed in the previous section, the TLS average position (and thus the emitted THz radiation) exhibits quenched oscillations. While the output THz radiation is not monochromatic, an oscillation at the natural tunneling frequency is a significant component of the generated field. Through the QSR phenomenon, one expects that the use of the THz radiation produced from the first DQW as a driving field on a second identical system will lead to a slower quenching of the induced TLS oscillations and thus to the generation of longer-lived radiation in the THz domain. This is indeed observed in our numerical calculations displayed in Fig. 7(b). Iteration of this procedure leads to further enhancement of the output radiation and can lead to the generation of THz fields with narrow frequency bands. Fig. 7 shows that the THz signal enhancement attainable from four iterations of the QSR driving process can be quite significant.

4. Concluding remarks

We have investigated the THz radiation emitted from excited double quantum wells using a dissipative harmonic bath to model the decoherence effects of intercarrier interactions. These decoherence effects lead to a quenching of the emitted THz signal within a few periods of oscillation. However, we have demonstrated that by using the emitted THz radiation from a given DQW to drive an identically prepared system, the oscillatory character of the THz signal can be enhanced. Repeating the procedure can lead to significant boosting of the emitted radiation.

These effects are a consequence of QSR. Our recent work revealed the existence of rich behaviors in the steady-state oscillation of a driven dissipative TLS that become more complex in the strong field regime. The strongly non-linear nature of this phenomenon leads to a variety of control possibilities. Because the strongest components of the output radiation from a DQW are in the vicinity of the natural tunneling frequency of the system, the radiation generated this way provides can be viewed as a zeroth order QSR driving field, broadened in frequency space as a result of dissipative intercarrier processes. As a result of its driving by an approximate QSR field, the second DQW responds by producing longer lived oscillations and thus a THz radiation field with a narrower frequency band. Iteration of this procedure was seen to lead to a significant boosting of the generated radiation. This QSR-induced enhancement of generated THz radiation can find a wide range of applications.

Acknowledgements

This work was supported by the National Science Foundation under award No. CHE-0212640.

References

[1] P.C.M. Planken, M.C. Nuss, I. Brener, K.W. Goossen, M.S.C. Luo, S.L. Chuang, L. Pfeiffer, Phys. Rev. Lett. 69 (1992) 3800.
[2] K. Leo, J. Shah, E.O. Goebel, T.C. Damen, S. Schmitt-Rink, W. Schaefer, K. Koehler, Phys. Rev. Lett. 66 (1991) 201.
[3] H.G. Roskos, M.C. Nuss, J. Shah, K. Leo, D.A. Miller, A.M. Fox, S. Schmitt-Rink, K. Koehler, Phys. Rev. Lett. 68 (1992) 2216.
[4] M.S.C. Luo, S.L. Chuang, P.C.M. Planken, I. Brener, M. Nuss, Phys. Rev. B 48 (1993) 4903, see also p. 11043.
[5] P.C.M. Planken, I. Brener, M.C. Nuss, M.S.C. Luo, S.L. Chuang, Phys. Rev. 48 (1993) 4903.
[6] R. Loefstedt, S.N. Coppersmith, Phys. Rev. Lett. 72 (1994) 1947.
[7] D.E. Makarov, N. Makri, Phys. Rev. B 52 (1995) R2257.
[8] M. Grifoni, P. Hänggi, Phys. Rev. Lett. 76 (1996) 1611.
[9] A. Buchleitner, R.N. Mantegna, Phys. Rev. Lett. 80 (1998) 3932.
[10] M. Grifoni, P. Hanggi, Phys. Rep. 304 (1998) 229.
[11] L. Gammaitoni, P. Hanggi, P. Jung, F. Marchesoni, Rev. Mod. Phys. 70 (1998) 223.
[12] Y. Nakamura, Y.A. Peshkin, J.S. Tsai, Phys. Rev. Lett. 87 (2001), art. no. 246601.
[13] T. Wellens, A. Buchleitner, Phys. Rev. Lett. 84 (2000) 5118.
[14] K. Dong, N. Makri, Phys. Rev. A (submitted).
[15] R.P. Feynman, J.F.L. Vernon, Ann. Phys. 24 (1963) 118.
[16] J.L. Krause, D.H. Reitze, G.D. Sanders, A.V. Kuznetsov, C.J. Stanton, Phys. Rev. B 57 (1998) 9024.
[17] W. Potz, Appl. Phys. Lett. 68 (1996) 2553.
[18] A.J. Leggett, S. Chakravarty, A.T. Dorsey, M.P.A. Fisher, A. Garg, M. Zwerger, Rev. Mod. Phys. 59 (1987) 1.
[19] R. Zwanzig, J. Stat. Phys. 9 (1973) 215.
[20] Makri, Chem. Phys. (submitted) (1998).
[21] N. Makri, D.E. Makarov, J. Chem. Phys. 102 (1995) 4600.
[22] N. Makri, J. Math. Phys. 36 (1995) 2430.
[23] E. Sim, N. Makri, Chem. Phys. Lett. 249 (1996) 224.
[24] E. Sim, N. Makri, Comp. Phys. Commun. 99 (1997) 335.
[25] N. Makri, J. Phys. Chem. 102 (1998) 4414.
[26] J. Shao, N. Makri, Chem. Phys. 268 (2001) 1.
[27] J. Shao, N. Makri, J. Chem. Phys. 116 (2002) 507.
[28] N. Makri, J. Chem. Phys. 111 (1999) 6164.
[29] N. Makri, L. Wei, Phys. Rev. E 55 (1997) 2475.
[30] P. Neu, R.J. Silbey, Phys. Rev. A 54 (1996) 5323.
[31] D.E. Makarov, Phys. Rev. E 48 (1993) R4146.
[32] J. Plata, J.M. Gomez Llorente, Phys. Rev. A 48 (1993) 782.
[33] P. Hanggi, P. Jung, C. Zerbe, F. Moss, J. Stat. Phys. 70 (1–2) (1993) 25.
[34] P. Jung, Phys. Rep. 234 (1993) 175.
[35] D.A.B. Miller, D.S. Chemla, T.C. Damen, A.C. Gossard, W. Wiegmann, T.H. Wood, C.A. Burrus, Phys. Rev. B 32 (1985) 1043.
[36] P.G. Huggard, C.J. Shaw, S.R. Andrews, J.A. Cluff, R. Grey, Phys. Rev. Lett. 84 (2000) 1023.